

A simulation study to examine the use of cross-correlation as an estimate of surface EMG cross talk

Madeleine M. Lowery,^{1,2} Nikolay S. Stoykov,^{1,2} and Todd A. Kuiken^{1,2,3}

¹Rehabilitation Institute of Chicago, and ²Department of Physical Medicine and Rehabilitation, Northwestern University, Chicago 60611; and ³Department of Electrical and Computer Engineering, Northwestern University, Evanston, Illinois 60208

Submitted 29 July 2002; accepted in final form 14 November 2002

Lowery, Madeleine M., Nikolay S. Stoykov, and Todd A. Kuiken. A simulation study to examine the use of cross-correlation as an estimate of surface EMG cross talk. *J Appl Physiol* 94: 1324–1334, 2003. First published December 6, 2002; 10.1152/jappphysiol.00698.2002.—Cross-correlation between surface electromyogram (EMG) signals is commonly used as a means of quantifying EMG cross talk during voluntary activation. To examine the reliability of this method, the relationship between cross talk and the cross-correlation between surface EMG signals was examined by using model simulation. The simulation results illustrate an increase in cross talk with increasing subcutaneous fat thickness. The results also indicate that the cross-correlation function decays more rapidly with increasing distance from the active fibers than cross talk, which was defined as the normalized EMG amplitude during activation of a single muscle. The influence of common drive and short-term motor unit synchronization on the cross-correlation between surface EMG signals was also examined. While common drive did not alter the maximum value of the cross-correlation function, the correlation increased with increasing motor unit synchronization. It is concluded that cross-correlation analysis is not a suitable means of quantifying cross talk or of distinguishing between cross talk and coactivation during voluntary contraction. Furthermore, it is possible that a high correlation between surface EMG signals may reflect an association between motor unit firing times, for example due to motor unit synchronization.

surface electromyography; model; synchronization

SURFACE ELECTROMYOGRAPHY (EMG) is a widely used tool for measuring muscle activity. One of its main advantages is the large pick-up volume of surface electrodes, which enables the behavior of a wide range of motor units to be studied. However, this also means that unwanted signals from muscles lying in the vicinity of the muscle fibers of interest may also be detected. These signals, known as myoelectric cross talk, are one of the most significant limiting factors currently associated with surface EMG. The problem of cross talk is further compounded by the difficulties associated with detecting and quantifying the volume-conducted signals. The most direct method of assessing cross talk is to examine surface signals detected at different sites

while selectively activating a single muscle. Mangun et al. (31) detected significant levels of EMG cross talk with fine-wire electrodes in denervated cat hindlimb muscles during a variety of motor tasks. De Luca and Merletti (12) examined EMG cross talk in the muscles of the leg while selectively stimulating the tibialis anterior muscle. Similarly, Koh and Grabiner (27) examined cross talk in the hamstrings while stimulating the quadriceps femoris. Both of these studies report volume-conducted EMG signals above regions of inactive muscle tissue with a root-mean-square (RMS) amplitude as high as 17% of that detected above the stimulated muscle. The results reported by Van Vugt and van Dijk (43) also reveal high levels of cross talk above the tibial, soleus, and gastrocnemius muscles during electrically elicited and voluntary contractions.

In practice, however, it is often difficult to selectively activate a single muscle. Results are also complicated by the possibility that reflex arcs may cause the activation of muscles other than those directly stimulated, leading to inaccurately high cross-talk estimates (40). Furthermore, it is not clear whether the results of electrical stimulation studies may be extended to voluntary contractions, due to the synchronous activation of motor units during electrical stimulation and the activation of different motor unit populations during voluntary and electrically elicited contractions.

Several authors have suggested that surface EMG cross talk can be detected during voluntary contraction by examining the cross-correlation of surface EMG signals detected above different muscles (29, 32, 45, 46). Specifically, it has been proposed that the square (R_{xy}^2) of the maximum value (R_{xy}) of the normalized cross-correlation function (R_{xy}) may be used to identify the common component between two signals, yielding a measure of EMG cross talk (45). While such a technique offers a potentially valuable means of quantifying cross talk, without necessitating the selective activation of single muscles, this method has been presented without any quantitative evaluation. Estimates of surface EMG cross talk based on cross-correlation values are substantially lower than values measured above similar muscles during electrical stimulation or selective voluntary activa-

Address for reprint requests and other correspondence: M. Lowery, Dept. of Physical Medicine and Rehabilitation, Northwestern Univ., Rehabilitation Institute of Chicago, Chicago IL 60611–4496 (E-mail: m-lowery@northwestern.edu).

The costs of publication of this article were defrayed in part by the payment of page charges. The article must therefore be hereby marked “advertisement” in accordance with 18 U.S.C. Section 1734 solely to indicate this fact.

tion (12, 27, 45). These differences have been attributed to variations in the techniques employed (45); however, it is well known that the action potential waveform changes as it propagates through different volumes of tissue due to spatial filtering of the propagating action potential. It is, therefore, not clear that the cross-correlation coefficient can provide a reliable indicator of EMG cross talk (12). It is also possible that a high correlation between surface EMG signals recorded above adjacent muscles could reflect a correlation in motor unit discharge patterns, rather than a common electrical source. Two distinct examples of correlated motor unit firing patterns that have been identified are common drive and short-term motor unit synchronization. Common drive is the term used to describe simultaneous fluctuations in the mean firing rates of different motor units (9, 11), whereas short-term synchronization refers to an increased tendency of motor units to fire within a few milliseconds of one another (36, 37). Recent studies have provided evidence for the existence of both common drive and motor unit synchronization between synergist muscle pairs acting about the same joint (4, 9, 33). Despite these concerns, the cross-correlation coefficient remains a commonly employed method of estimating surface EMG cross talk and is often used as a means of distinguishing between cross talk and coactivation of neighboring muscles (1, 6, 18, 41).

In this paper, the relationship between cross talk and the cross-correlation of surface EMG signals is examined by using model simulation. The model enables selective stimulation of different regions of muscle under conditions in which the inputs to the system, including the locations of the active motor units, are known. The model is based on a finite-element model of surface EMG in an idealized cylindrical limb (30). The aim of the study is to estimate surface EMG cross talk during voluntary and electrically stimulated contractions and to explore whether the cross-correlation function provides a reliable estimate of cross talk. The effect of both common drive and motor unit synchronization on the cross-correlation of surface EMG signals is also examined. The complexity of the problem is compounded by the inhomogeneous nature of the volume conductor due to differences in the electrical prop-

erties of muscle, fat, and skin tissue. Cross talk and cross-correlation are, therefore, examined for different subcutaneous fat thicknesses.

METHODS

EMG Model

EMG signals were simulated by using a finite-element model of an idealized cylindrical limb composed of bone, muscle, fat, and skin tissue, described in Ref. 30. Finite-element analysis is a numerical technique, which enables the electric field to be solved within inhomogeneous and nonsymmetric geometries. Fat and skin tissues have previously been incorporated into surface EMG models with the use of analytic methods (21, 24, 34). A bone of 10-mm radius was placed at the center of the volume conductor, surrounded by cylindrically anisotropic muscle of 40-mm radius and a layer of fat tissue. Three thicknesses of subcutaneous fat were simulated, 3, 9, and 18 mm. The fat tissue was surrounded by a layer of skin, 1.3 mm thick (39). Pairs of bipolar electrodes were positioned radially around the skin surface at intervals of 7.5° (Fig. 1A). The electrodes were simulated as point electrodes and arranged in bipolar pairs, 20 mm apart, orientated along the direction of the muscle fiber.

The surface of the volume conductor was covered in a uniform, high-resolution rectangular mesh. The conducting volume was then divided into sets of linear tetrahedral elements. Elements of a very small size were used to mesh the areas surrounding the regions of interest to facilitate a high level of accuracy where required, whereas a coarser resolution was used elsewhere in the model. Unique material properties were defined for each element set, corresponding to different tissues within the model. The electric potential at the vertices of the elements was calculated by using the finite-element method, assuming that the volume conductor was infinite in length. The finite-element model was meshed and solved by using the EMAS software package (Ansoft, Pittsburgh, PA).

Single-fiber action potential. The transmembrane current density was represented by a series of 150 current sources obtained by discretizing the second derivative of the transmembrane voltage, described analytically by Rosenfalck (35). The current source was located symmetrically between the two ends of the model and orientated parallel to the skin surface.

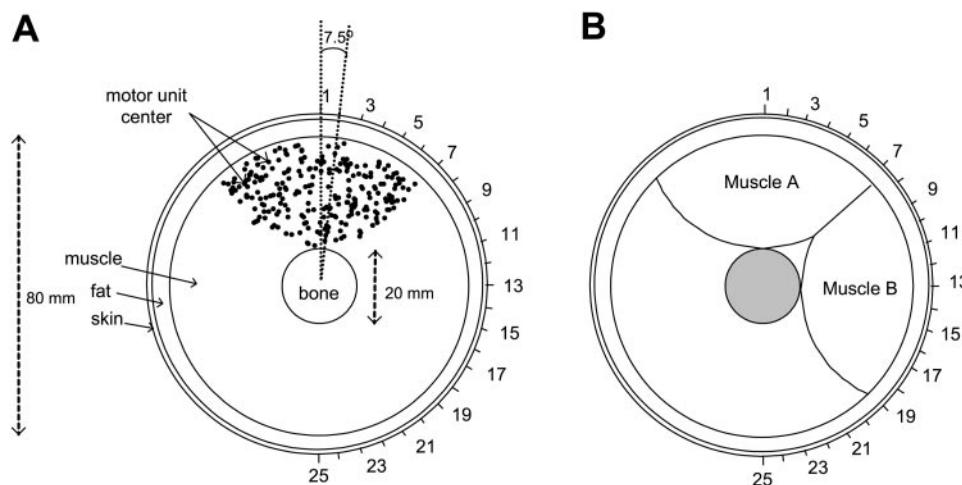


Fig. 1. Cross-section of electromyography (EMG) model. A: single-muscle model, indicating random location of 350 motor units and the radial position of 25 surface electrode pairs. B: location of muscles A and B in the volume conductor model.

Action potential startup and end effects were incorporated by means of current compensation at the fiber end plate and terminations, which ensured that the sum of the total current along the fiber was always equal to zero (24). To implement these effects, a weighting function was calculated for each fiber and electrode location, which represented the impulse response of the model for a fiber of infinite length (13). The compensation currents were then applied by multiplying the integral of the current along the fiber by the weighting function at the fiber termination, at extinction of the action potential, and at the fiber end plate at the action potential generation, and subtracting the resultant potential from that due to the propagating action potential. This was repeated for action potentials propagating in both directions away from the fiber end plate. The implementation of the end effects in this manner is similar to that described by Duchene and Hogrel (16).

Two muscle fiber lengths were simulated, a fiber length of 300 mm, corresponding to the biceps brachii (47), and a shorter fiber length of 100 mm. It was assumed that all fibers ran the entire length of the muscle, parallel to one another. The muscle fiber end plates were randomly distributed throughout a region 5 mm wide, located at the center of the fiber length. The fiber terminations were similarly distributed throughout a 5-mm-wide region at either end of the muscle. In the case of the 300-mm fibers, the bipolar electrodes were placed 80 and 60 mm from the center of the end-plate zone, whereas, for the 100-mm-long fibers, the electrodes were placed 15 and 35 mm from the center of the end-plate zone, halfway between the end-plate zone and the tendon. Examples of surface action potentials detected at different electrodes for a fiber located 5 mm below the surface of the muscle with a 9-mm-thick fat layer are presented in Fig. 2. Data are shown for 300- and 100-mm fibers with monopolar and bipolar electrode configurations.

Extracellular potentials were calculated for muscle fibers located at 15 depths below the surface of the muscle (Table 1). The potential on the skin surface at increments of 2.5° from the vertical axis was calculated for each muscle fiber. Due to the symmetry of the volume conductor, this yielded a series of action potentials representing surface potentials generated by fibers located at each depth, at multiples of 2.5° from the vertical axis, yielding a total of 2,160 action potentials ($15 \text{ depths} \times 360/2.5$ angular positions). A database of surface potentials was generated for each model. Details of the model parameters are given in Table 1, and further details of the finite-element model may be found in Ref. 30.

Motor unit distribution. Each muscle contained 350 motor units randomly distributed throughout an area of 30-mm radius centered on the intersection of the muscle and fat tissue. Two separate muscles were defined. The first muscle, denoted *muscle A*, was located directly below *electrode 1* (Fig. 1A). A second muscle of equal size and shape, denoted *muscle B*, was located adjacent to *muscle A* (Fig. 1B). The simulated muscle fiber, which lay closest to each randomly located motor unit, was identified, and it was assumed that all fibers in the motor unit were located at this cross-sectional location. Motor unit action potentials were then generated by summing together a series of single-fiber action potentials. The fibers in each motor unit were identical, except in the location of the end plates and terminations, which introduced a temporal dispersion between the single-fiber action potentials in each motor unit action potential.

The properties of the motor unit pool were assumed to be the same for both muscles. The mean number of muscle fibers innervated by a single motoneuron has been reported to be in excess of 410 in the brachioradialis muscle (22) and 750 in the biceps brachii (5). Although the distribution of the innervation ratio is not yet well established in human muscles, it appears that many units produce a small force, whereas

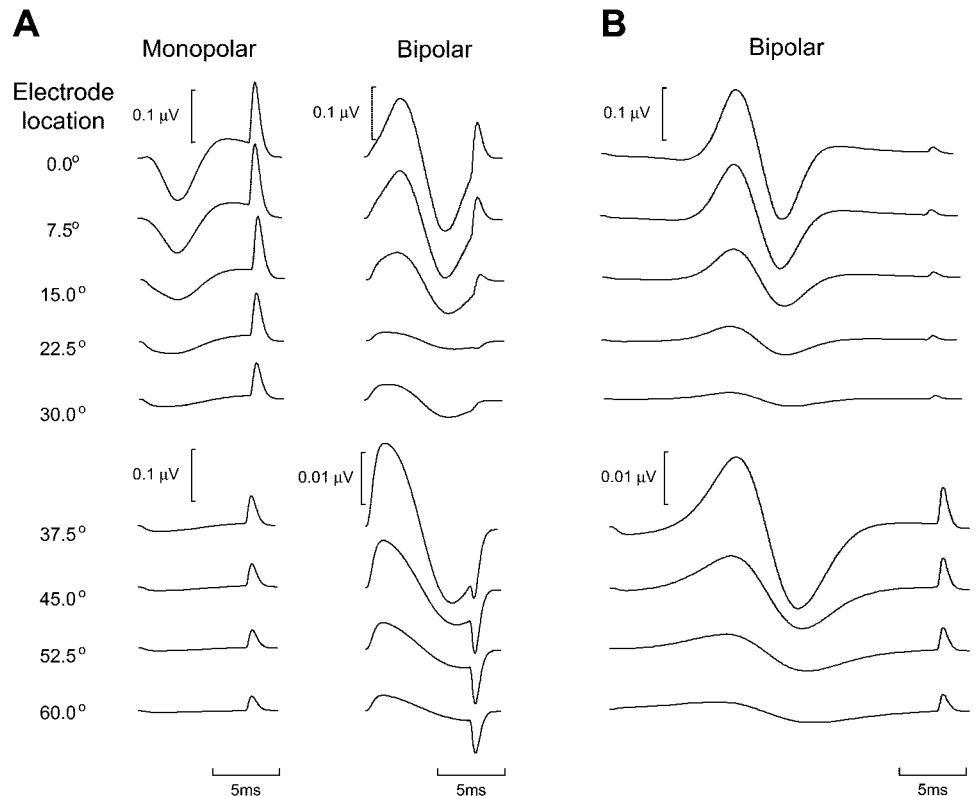


Fig. 2. Simulated surface action potentials generated by a muscle fiber 5 mm below the muscle-fat interface, with a fat thickness of 9 mm. A: action potentials from a 100-mm-long muscle fiber are presented for a monopolar electrode located 15 mm from the center of the end-plate zone and for bipolar electrodes 15 and 35 mm from the end-plate zone. B: action potentials are also presented for a 300-mm-long muscle fiber. Note the change of amplitude scale for bipolar recordings detected further from the fiber.

Table 1. *Model parameters*

Model Parameter	Value	Reference
Radius of bone tissue, mm	10	25
Radius of muscle tissue, mm	40	
Subcutaneous fat thickness, mm	3, 9, 18	17
Skin thickness, mm	1.3	39
Muscle conductivity in transverse direction, σ_t , S/m	0.2455	23
Skin conductivity, σ_s , S/m	4.55×10^{-4}	23
Fat conductivity, σ_f , S/m	0.0379	23
Cortical bone conductivity, σ_b , S/m	0.02	23
Intracellular conductivity, σ_i , S/m	1.01	3
Muscle anisotropy ratio, λ	5	3
Muscle fiber diameter (d), μm	50	5
Transmembrane voltage [$v_m(z)$]	$v_m(z) = 96z^3 e^{-z} - 90$	35
Source length, mm	15	
Muscle fiber length, mm	300, 100	47
Muscle fiber conduction velocity (u), m/s	3.5–4.5	19
Mean motor unit firing rate, Hz	15–25	
Interpulse interval SD about mean ($\overline{\text{IPI}}$), ms	$\text{SD} = 9.1 \times 10^{-4} \overline{\text{IPI}}^2 + 4$	7
Simulated muscle fiber depths – distance below muscle surface, mm	1, 2, 3, 4, 5, 6, 7, 8, 10, 12.5, 15, 17.5, 20, 25, 27.5	

relatively few produce a large force, predominantly due to variations in the number of fibers per unit (20). The number of muscle fibers in each motor unit was, therefore, simulated to increase exponentially from 428 to 700, such that the mean number of fibers per motor unit was 516 and the muscle contained a total of 190,150 fibers. All fibers were simulated with a diameter of 50 μm (5), and muscle fiber conduction velocity was uniformly distributed between 3.5 and 4.5 m/s, with the lowest conduction velocity assigned to the smallest motor unit (2, 19).

Simulated voluntary EMG. Mean motor unit firing rates ranged linearly with a constant step size from 15 to 25 Hz. The motor unit interpulse intervals (IPIs) were generated to have a Gaussian distribution about the mean IPI (7) (Table 1). The coefficient of variation (ratio of the standard deviation to the mean) of the IPIs ranged from 0.12 to 0.13, which lies within the range of values reported for the biceps brachii of 0.11–0.14 (15). Trains of motor unit action potentials were generated in this manner to represent the successive firing of each unit within the muscle. The motor unit action potential trains were then summed to yield the surface EMG signal at each electrode. EMG signals were simulated at a sampling rate of 2 kHz.

Surface EMG signals were first examined for a single active muscle, *muscle A*, and then when adjacent *muscles A* and *B* were simultaneously active (Fig. 1B). Equal numbers of motor units were activated at each firing rate in both muscles. EMG signals were simulated under three different conditions: independent activation of both muscles, common drive applied simultaneously to both muscles, and synchronization between the firings of motor units in both muscles.

Simulation of common drive. Experimental studies have reported common drive in the form of significant in-phase fluctuations of the firing rates of motor units in pairs of muscles during both antagonist and synergist muscle coactivation (9, 10). It has been suggested that cross-talk estimates based on the cross-correlation of surface EMG signals may be affected by the presence of common drive to both muscles (12). To investigate possible effects of common drive on the cross-correlation of surface EMG signals during coactivation of neighboring muscles, a 1-Hz sinusoidal term was added to the mean firing rate of all motor units in *muscles A* and *B*. The amplitude of the sinusoidal term was equal to 5%, and then 10%, of the mean firing rate of each motor unit. A delay of 34 ms was introduced between the firing rate modulation

applied to the two muscles in accordance with experimental observations (9). To examine whether the simulated common firing rate fluctuations were consistent in magnitude with those observed experimentally, the smoothed, time-varying, mean firing rates of motor units from the two muscles were correlated with one another as described in Refs. 9 and 11. The mean value of the resulting maximum mean firing rate cross-correlation, calculated from 49 pairs of simulated motor units with a common signal equal to 5% of each mean motor unit firing rate, was 0.53 ± 0.10 , which compares with a reported value of 0.46 ± 0.10 between the firings of motor units in the extensor carpi radialis longus and the extensor carpi ulnaris, with both muscles acting synergistically (9).

Simulation of intermuscular motor unit synchronization. To examine whether short-term synchronization can alter the cross-correlation between EMG signals recorded over different muscles, motor unit synchronization was incorporated based on the model described by Yao et al. (48). A sequence of firing times was first generated for each active motor unit. The firing times of a proportion of randomly chosen motor units were then synchronized with a proportion of the firing times of a single reference unit. This was repeated for all motor units in *muscle A*, so that each served as a reference against which a proportion of the firings of a randomly selected group of motor units from *muscles A* and *B* was synchronized. The discharges of first 5% and then 10% of motor units from *muscles A* and *B* were synchronized with 5% and 10%, respectively, of the firings of each motor unit in *muscle A*. The amount of motor unit synchronization was quantified by using the population synchrony index (PSI) proposed by Yao et al. (48) and similarly used by Kleine et al. (26). The PSI provides a measure of the amount of synchronization throughout the motor unit population by calculating the difference between the total number of coincident impulses and the total number of coincident impulses expected due to chance based on a Poisson distribution, before normalizing with respect to the latter number (48). The PSI was calculated at each synchronization level by calculating the total number of coincident impulses across all active motor units in bins of 1-ms duration. Synchronization at the 5% level yielded a mean PSI value of 0.17 (SD 0.013), whereas synchronization at the 10% level yielded a mean PSI value of 0.89 (SD 0.045), averaged over 20 simulations. A PSI of 0.94 has been reported to correspond to a moderate level of synchrony for motor units within a single muscle (48).

Simulated electrically elicited EMG. The surface EMG signal was examined as all motor units in a single muscle were simultaneously activated as in electrically elicited contractions. The temporal dispersion of individual motor unit action potentials due to variations in motor axon conduction velocities, terminal branch lengths, and variations in the neuromuscular delay was incorporated as variations in the distribution of the motor unit end plates and in the muscle fiber conduction velocities. It was assumed that all motor units within the muscle were activated.

Processing of Simulated Data

The choice of motor unit size, fiber diameter, and conduction velocity distributions implemented in the model is somewhat arbitrary due to the limited information available. Different motor unit distributions will alter the EMG distribution at the skin surface. For this reason, the following EMG parameters were calculated from 20 sets of simulated data, each conducted with a different set of randomly located motor units. In Figs. 2–8, data are presented as the means of 20 simulations, whereas the mean and standard deviations are given in Table 2.

Cross-talk index. Cross talk was defined as the RMS value of the EMG signal at each electrode, normalized with respect to the EMG RMS value directly above the center of the active muscle, during selective activation of that muscle. The RMS value of 1 s of simulated EMG data at each bipolar electrode pair was calculated and normalized with respect to the EMG signal detected at *electrode 1* (Fig. 1A).

Cross-correlation index. The raw EMG signal at each electrode was repetitively correlated with the signal at *electrode 1* while the time delay was successively increased between the two signals. The cross-correlation function was normalized with respect to the autocorrelation of both signals at zero time lag (44, 46), and the \bar{R}_{xy} was determined (Fig. 3B). It has been proposed that the proportion of cross talk between two EMG signals is given by the \bar{R}_{xy}^2 (46). The value of \bar{R}_{xy}^2 , which will be referred to here as the cross-correlation index, was compared with the EMG cross-talk index defined above.

Median frequency of EMG power spectrum. The power spectrum of an epoch of EMG data, 1 s in duration (2,000 samples), was calculated at each electrode location. The

power spectrum was obtained by calculating the discrete Fourier transform of the autocorrelation function of the EMG signal. The median frequency of the power spectrum, defined as the frequency below which one-half of the power in the EMG signal lies, was then calculated for each simulated EMG signal.

Statistical analysis of simulation results. Mean values of groups of EMG variables, calculated from data simulated under different conditions, were subjected to a one-way ANOVA. The data were then analyzed by using a Scheffé's post hoc test to detect differences between groups. A probability of the null hypothesis being true (P) of <0.05 ($P < 0.05$) was taken as indicating a statistically significant difference between groups.

RESULTS

Single Active Muscle

An example of simulated surface EMG signals detected at *electrodes 1, 5, and 9*, with a 9-mm-thick subcutaneous fat layer and 300-mm fiber length, is presented in Fig. 3A. The amplitude of each signal has been normalized with respect to the RMS value at *electrode 1*. The \bar{r}_{xy} between the EMG signal detected at each electrode and the signal detected at *electrode 1* is presented in Fig. 3B.

Values for EMG cross talk (normalized RMS value), the cross-correlation index (\bar{R}_{xy}^2), and the normalized median frequency of the EMG power spectrum are compared in Fig. 4 for three different thicknesses of fat tissue and for two different muscle fiber lengths. The amplitude of the EMG signal remained relatively constant above the active muscle fibers, decaying as the observation point was moved away from the edge of the muscle (Fig. 4, A and D). In contrast, the \bar{R}_{xy} began to decrease once the observation point was moved away from the reference electrode (Fig. 4, B and E). For the longer muscle fibers, the median frequency of the EMG power spectrum remained relatively constant above the active fibers, decaying as the observation point was

Table 2. EMG cross-talk, cross-correlation index and median frequency for simulated voluntary activation of muscle A

Electrode Location	Cross-talk Index, Normalized RMS, %		Cross-correlation Index, \bar{R}_{xy}^2 , %		Median Frequency, Hz	
	300-mm fiber	100-mm fiber	300-mm fiber	100-mm fiber	300-mm fiber	100-mm fiber
<i>3-mm Fat layer</i>						
1	100.0 ± 0	100.0 ± 0	100.0 ± 0	100 ± 0	119.1 ± 5.7	126.7 ± 4.7
5	100.2 ± 32.8	103.1 ± 26.4	1.6 ± 0.3	1.7 ± 0.3	118.3 ± 7.6	125.2 ± 6.2
9	6.5 ± 1.7	6.8 ± 1.5	1.0 ± 0.2	1.1 ± 0.3	61.4 ± 5.8	68.4 ± 3.5
13	0.7 ± 0.1	0.9 ± 0.2	0.3 ± 0.1	0.9 ± 0.3	24.3 ± 1.7	68.9 ± 4.5
<i>9-mm Fat layer</i>						
1	100.0 ± 0.0	100.0 ± 0.0	100.0 ± 0	100.0 ± 0	76.4 ± 2.1	85.6 ± 3.6
5	98.0 ± 14.1	102.7 ± 12.6	7.2 ± 2.1	7.3 ± 2.2	77.1 ± 3.4	86.2 ± 3.0
9	23.1 ± 4.1	25.1 ± 3.2	2.5 ± 0.6	2.2 ± 0.6	57.4 ± 3.2	66.0 ± 2.5
13	2.8 ± 0.3	3.5 ± 0.4	1.5 ± 0.3	2.3 ± 0.7	25.8 ± 2.7	62.1 ± 2.8
<i>18-mm Fat layer</i>						
1	100.0 ± 0.0	100.0 ± 0.0	100.0 ± 0	100.0 ± 0	65.0 ± 2.6	67.9 ± 3.4
5	93.7 ± 5.8	97.5 ± 11.2	18.0 ± 4.5	22.2 ± 4.7	63.7 ± 2.8	68.0 ± 3.7
9	29.4 ± 1.8	36.5 ± 5.3	4.9 ± 2.1	7.3 ± 2.7	49.0 ± 2.7	58.8 ± 2.8
13	5.4 ± 1.0	7.4 ± 0.9	3.9 ± 2.0	6.7 ± 2.0	25.6 ± 2.5	62.1 ± 2.8

Values are means ± SD of 20 simulations. RMS, root mean square; \bar{R}_{xy}^2 , the square of the maximum value of normalized cross-correlation.

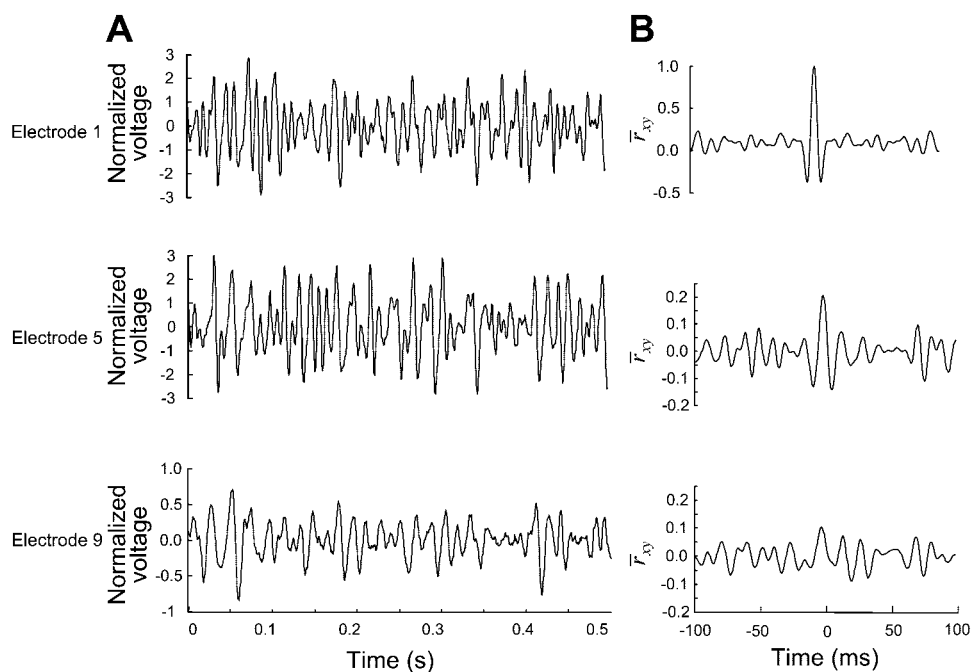


Fig. 3. Simulated surface EMG data. *A*: EMG signals detected at electrode locations 1, 5, and 9, with bipolar electrodes 20 mm apart. The subcutaneous fat layer was 9 mm thick, and the fiber length was 300 mm. The data have been normalized with respect to the EMG root-mean-square (RMS) amplitude at *electrode 1*. *B*: normalized cross-correlation (\bar{r}_{xy}) between the EMG signal detected at each electrode and that detected at *electrode 1*.

moved above the inactive muscle tissue (Fig. 4C). However, with the shorter fiber length, the median frequency decreased slightly as the electrodes were moved above the inactive tissue initially but then began to increase as the electrodes were moved progressively further away (Fig. 4F). Similar results were observed when the electrodes were placed close to the end of the 300-mm fibers.

The rate at which all three variables decayed around the surface of the model decreased as the subcutaneous fat thickness increased. ANOVA confirmed a statistically significant effect of fat thickness on the RMS-based cross-talk index at all electrodes lying above the inactive muscle tissue (*electrodes 8–25*, Fig. 1; all $P < 0.001$). Post hoc testing revealed pairwise differences between cross-talk levels compared across all combinations of fat thicknesses at each of these electrodes, for the 100-mm fiber length. For the 300-mm fiber length, there were significant differences between cross talk with a 3-mm fat layer and both a 9- and 18-mm layer at *electrode 8* and between cross-talk values for all combinations of fat thicknesses at each of the other electrodes. The effect of fat thickness on the cross-correlation index was also statistically significant at all electrodes (excluding *electrode 1*), regardless of fiber length (all $P < 0.001$), with significant differences between the values of the cross-correlation index across all paired combinations of fat thicknesses at these electrodes (Scheffé's post hoc test comparison). The means and standard deviations of the cross talk, power spectrum median frequency, and cross-correlation index at *electrodes 1, 5, 9, and 13* are presented in Table 2.

In the following sections, results are presented for a fiber length of 300 mm and a 9-mm fat layer, as similar results were also observed with shorter fibers and 3- and 18-mm-thick fat layers.

Coactivation of Adjacent Muscles

The \bar{R}_{xy} , between the EMG signal at *electrode 1* and at each other electrode location, was calculated for several conditions of simultaneous activation of *muscles A and B*. Cross-correlation values during independent activation of both muscles and during the addition of a simultaneous common drive to both muscles are presented in Fig. 5. Neither the activation of the second muscle nor simultaneous modulation of mean motor unit firing rates with a 1-Hz common signal had a statistically significant effect on the maximum value of the cross-correlation function (Fig. 5).

Synchronization between the firings of motor units in the two muscles caused a substantial increase in the \bar{R}_{xy} . Simulated surface EMG signals and the normalized cross-correlation between the EMG signal detected at *electrode 1* and at *electrodes 5, 9, and 13* are presented in Fig. 6 for synchronization between motor units at the 5% level. The maximum value of the cross-correlation function is presented in Fig. 7 for both synchronization levels and for independent activation of both muscles.

The surface EMG signal at each electrode was examined as all motor units in *muscle A* were synchronously activated, similar to the electrically elicited activation of all motor units. The maximum value of the cross-correlation of the signal detected at each electrode and that detected at *electrode 1* is presented in Fig. 8, along with the normalized RMS value.

DISCUSSION

Surface EMG Cross Talk

Surface EMG cross talk has been examined by using a multiple-layer model of an idealized cylindrical limb. The simulation results confirm that significant levels

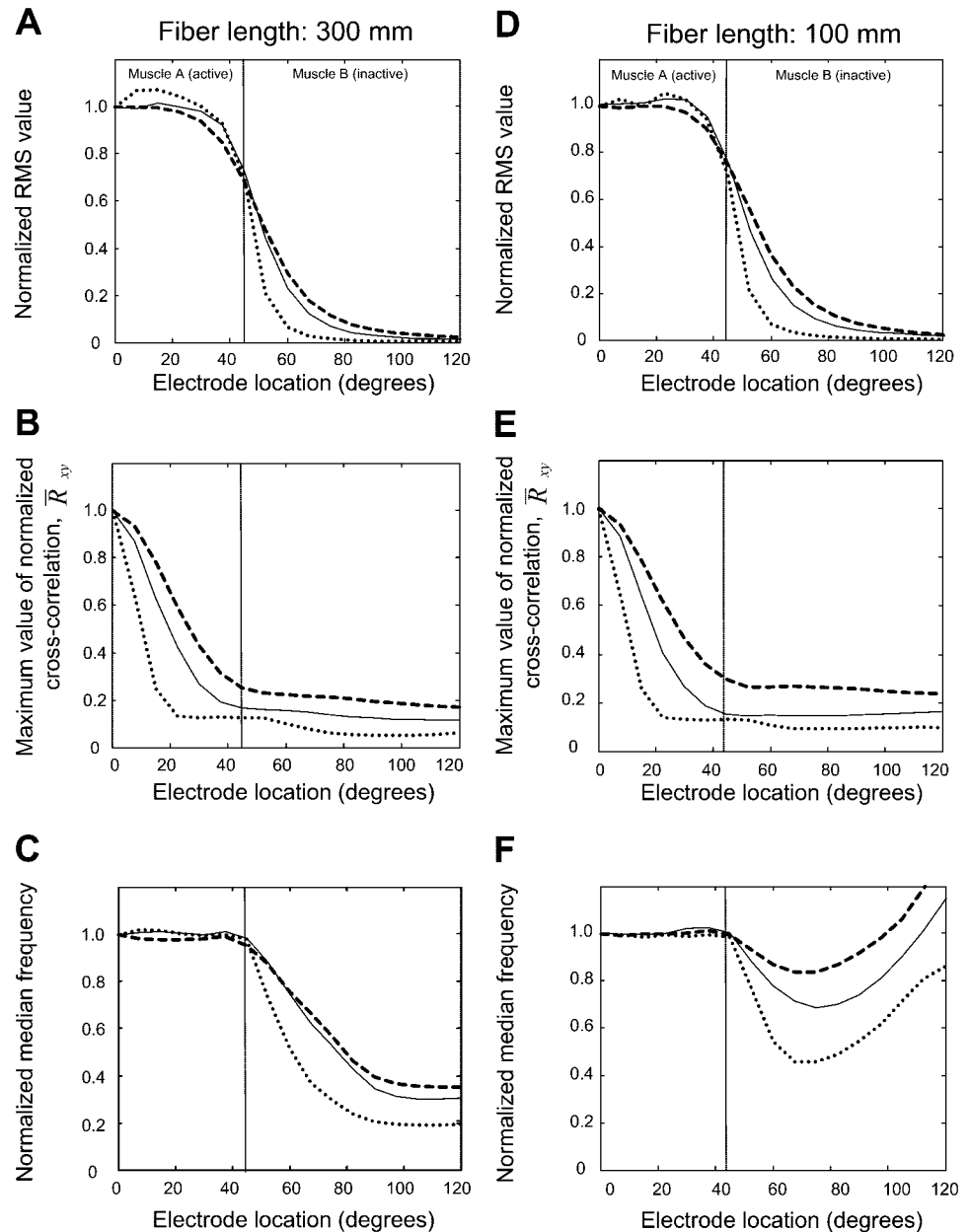


Fig. 4. Comparison of surface EMG parameters at different electrode locations for a single active muscle. Simulations have been performed for fiber lengths of 300 mm (A, B, and C) and 100 mm (D, E, and F). A and D: surface EMG cross talk (RMS value normalized with respect to the RMS value at *electrode 1*). B and E: maximum value of the normalized cross-correlation (\bar{R}_{xy}) between the EMG signal at each electrode and at *electrode 1*. C and F: median frequency of the EMG signal at each electrode normalized with respect to *electrode 1*. Data are presented for 3- (dotted line), 9- (solid line), and 18-mm-thick (dashed line) fat layers. The edge of *muscle A* is indicated with a vertical line.

of cross talk can be detected above inactive muscle tissue located close to an active muscle. Surface EMG cross talk increased with subcutaneous fat thickness (Table 2 and Fig. 4, A and D), consistent with reported experimental observations (8, 40). Based on simulation studies of a single muscle fiber, it appears that the increase in cross talk with subcutaneous fat thickness is due to the increased distance between the source and electrode, rather than the more resistive nature of the fat tissue relative to muscle (30).

Power Spectrum Median Frequency

The behavior of the EMG median frequency with increasing distance from the active fibers depended on the distance between the electrodes and the musculotendinous junction. The EMG signal generated by the

longer muscle fibers was dominated by the propagating waveforms, the spatial filtering of which causes the median frequency to decrease as the electrode is moved farther from the active muscle (Fig. 4C). However, with a shorter fiber length, the nontraveling muscle fiber end effects tended to dominate the signal at locations far from the source. As a result, the median frequency decreased slightly and then began to increase as the observation point was moved away from the active fibers (Fig. 4F). This result is in agreement with a recent study by Dimitrova et al. (14), who illustrated that action potentials from far-away motor units can be dominated by the muscle fiber end effects. Their conclusion that temporal high-pass filtering is not a suitable means of reducing cross talk is confirmed for conditions in which the muscle fiber end effects domi-

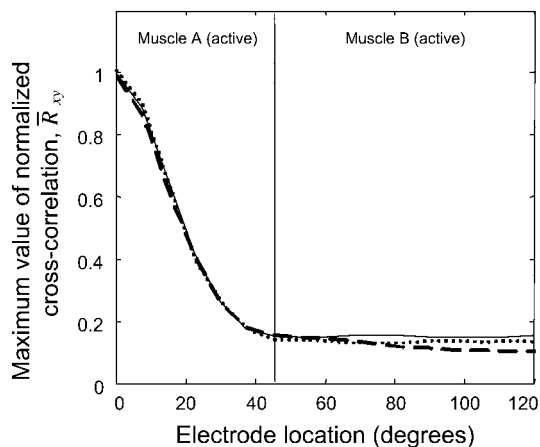


Fig. 5. Influence of simulated common drive on the cross-correlation between surface EMG signals during simultaneous activation of muscles A and B. The \bar{R}_{xy} between the signal at *electrode 1* and at each other electrode location is presented for independent activation of both muscles (solid line) and for sinusoidal firing rate modulation (common drive) applied to all motor units, equal in magnitude to 5% (dotted line) and 10% (dashed line) of each mean motor unit firing rate. Data are presented for a 9-mm-thick fat layer and a fiber length of 300 mm.

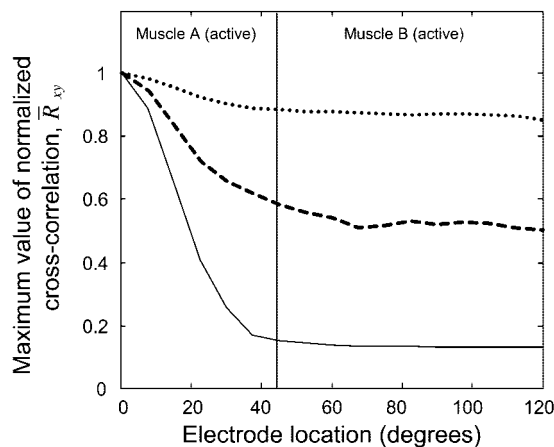


Fig. 7. Influence of motor unit synchronization on the cross-correlation between surface EMG signals. The \bar{R}_{xy} between the EMG signal at each electrode and at *electrode 1* was calculated as the motor units in muscles A and B were synchronized at the 5% (dashed line) and 10% (dotted line) synchronization levels, and for simultaneous independent activation of both muscles (solid line). Data are presented for a subcutaneous fat layer 9 mm thick and 300-mm fiber length.

nate the EMG signal. Lower center frequencies for cross-talk signals than for EMG signals from muscles below the electrodes have been reported in canine diaphragm muscles (38). Nevertheless, the simulations indicate that spectral parameters such as the median frequency are not a robust means of distinguishing between volume-conducted signals from distant muscles and EMG signals originating in muscles beneath the electrodes.

Cross-correlation as an Estimate of Surface EMG Cross Talk

From a comparison of the cross-talk and cross-correlation indexes across all electrode sites, it is concluded

that the cross-correlation function is not a suitable means of quantifying surface EMG cross talk or of distinguishing between cross talk and coactivation of neighboring muscles. Whereas the amplitude of the surface EMG signal remained relatively constant above the active muscle, the maximum value of the cross-correlation function began to decay once the observation point was moved away from the reference electrode. Furthermore, the cross-correlation index remained close to its minimum value as the surface EMG cross talk varied across a wide range of values (Fig. 4). For example, it may be seen that, although the cross-correlation index at *electrode 9* is very low (2.2–2.5%) for the 9-mm fat layer, significant levels of cross talk

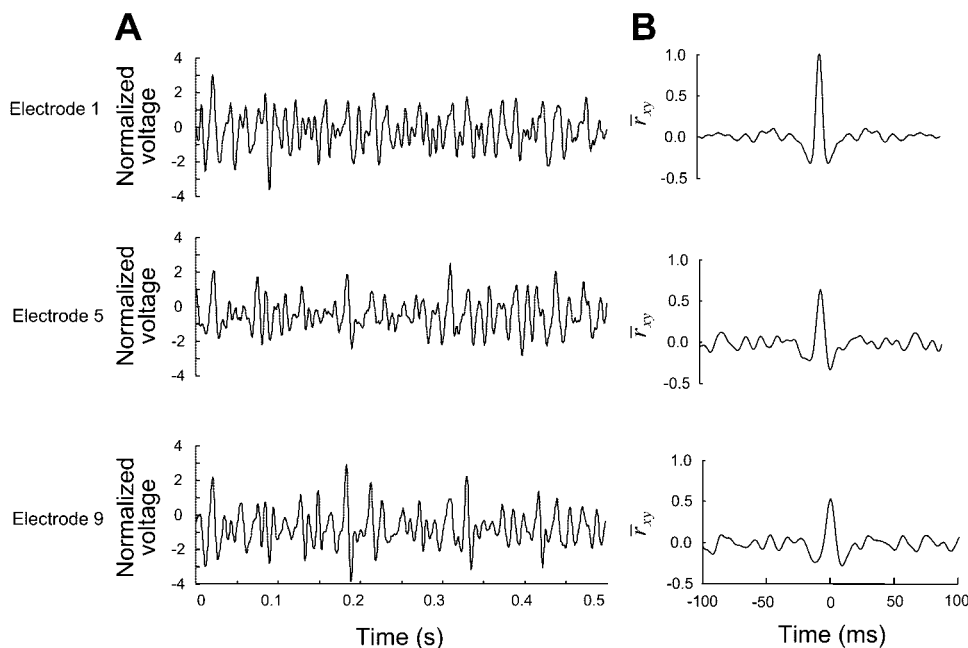


Fig. 6. A: EMG signals detected at electrode locations 1, 5, and 9, with bipolar electrodes 20 mm apart, with both muscles active and synchronization between the firing of motor units at the 5% level. The data have been normalized with respect to the EMG RMS amplitude at *electrode 1*. B: \bar{r}_{xy} between the EMG signal detected at each electrode and that detected at *electrode 1*. The subcutaneous fat layer was 9 mm thick, and the fiber length was 300 mm.

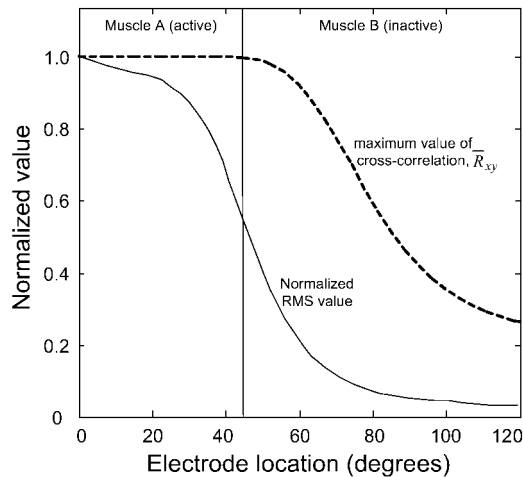


Fig. 8. \bar{R}_{xy} (dashed line) and normalized EMG RMS value (solid line) during simulated electrically elicited contraction. Data are presented for a 9-mm-thick fat layer and 300-mm fiber length.

(23–25%) were present (Table 2). A reliance on the cross-correlation index as an indicator of cross talk would lead to the erroneous conclusion that the EMG signal detected at this electrode is due to activation of the underlying muscle and contains negligible amounts of cross talk from the neighboring muscle.

The surface EMG signal during voluntary contraction may be modeled as a multiple-input, single-output linear system. It is, therefore, not possible to determine individual motor unit firing times by observing the EMG signal at a single site nor to predict the behavior of one EMG signal based on changes observed at another location when many motor units are active. The behavior of a small number of motor units may dominate the EMG signal at one electrode site, whereas the EMG signal at another site may be determined by another group of closer motor units. A low correlation was, therefore, observed between EMG signals at different electrode locations, even when both signals originated from motor units within the same muscle (Fig. 4, B and E). The weak correlation shows that the two EMG signals are not linearly related but does not indicate whether both have originated from the same combination of electrical sources. Although it is not clear what technique may provide an alternative means of detecting cross talk, spatial filtering of the surface EMG signal using double-differential or branched electrodes has been shown to reduce cross talk in experimental studies (12, 28, 43).

Influence of Common Drive

When two adjacent muscles were independently activated, the surface EMG signals above both remained weakly correlated, even at electrode sites at which the level of cross-contamination was high (Fig. 5). The addition of a limited amount of common drive to both muscles did not alter the maximum value of the cross-correlation, as the instances of motor unit firing remained unrelated, even though the mean firing rates were modulated according to a similar pattern (Fig. 5).

Influence of Synchronization

Short-term synchronization resulted in an increase in the correlation between surface EMG signals (Figs. 6 and 7). The increased cross-correlation values are due to the combined synchronization of units within the first muscle and between units across both muscles. Introducing synchronization between the firings of motor units across the two muscles, without synchronization of the motor units within the first muscle, alters the correlation between the two surface EMG signals by very little, as the structure introduced by synchronization is no longer present in the signal detected above the first muscle. The amount of synchronization throughout the motoneuron pool, quantified using the PSI, was comparable with levels used in similar EMG models (26, 48). The high correlation observed may indicate that these levels of synchronization are higher than what occurs experimentally. Alternatively, it may suggest that cross-correlation of surface EMG signals could be a useful indicator of synchronization between muscles where cross talk is not a contributing factor.

When the firings of all motor units are perfectly synchronized, or if a single motor unit is active, the EMG signal may be considered as a single-input, single-output system. In this case, there will be a deterministic relationship between EMG signals detected at different locations. This is reflected in the increase in the maximum value of the cross-correlation function with increasing motor unit synchronization (Fig. 7) and in the high correlation observed in the case of complete synchronization whereby all motor units fired simultaneously (Fig. 8). Similar results would be observed if there were no variation in the action potentials detected at different electrodes from a single source, which explains the increase in the cross-correlation index with increasing subcutaneous fat thickness.

Model Parameters

Skin has been modeled as a homogeneous structure by using the conductivity for skin moistened with deionized water measured in vivo by Gabriel et al. (23), using a coaxial probe with a penetration depth of 1–2 mm. In reality, skin is a complex, laminar structure. The dielectric properties measured represent values for composite skin that lie between the values for the highly resistive stratum corneum and the more conductive tissue of the dermis, which is significantly more hydrated and has a rich network of structures (23). In recent simulation studies, skin has been chosen to have a higher conductivity than fat or muscle tissue (21, 26, 34), based on observations that a highly conductive layer was necessary to explain the lateral spread of the EMG signal measured experimentally (34). Although the effects of skin tissue are not yet fully understood, it is clear that the choice of skin conductivity affects the rate at which the EMG signal decays, which has important implications in determining cross-talk levels. A more conductive skin tissue would

yield even higher estimates of EMG cross talk. The bounded nature of the volume conductor and the different conductivities of muscle, fat, skin, and bone tissue are also important factors in determining the extracellular potential, and thus cross talk, at different locations around the limb. The transmembrane action potential has been represented by a triphasic, multipole source, for which the extracellular potential decays more rapidly with increasing distance from the source than for the dipole source, which has been employed in previous cross-talk models (46). In accordance with previous studies, it has been assumed that biological tissues behave as if they were purely resistive at the frequencies of interest. It is possible, however, that other combinations of conductivity and permittivity may yield more significant capacitive effects (42). Inhomogeneities within each of the tissues, non-uniformity of the limb geometry, and variations in muscle fiber alignment could further alter volume conduction of the signal. Furthermore, whereas simulations indicate that bone located at the center of the generalized upper arm model has a negligible effect on the surface EMG signal, if the bone is located closer to the skin surface and to the active muscle fibers, it can cause a considerable distortion of the distribution of the EMG signal at the skin surface (30).

Conclusion

The simulation results presented question the validity of algorithms that seek to estimate EMG cross talk based on an assumption of a linear relationship between EMG signals detected at different electrode sites. The results suggest that the cross-correlation between two EMG signals is neither a qualitative nor quantitative measure of cross talk. It is, therefore, not a suitable means of distinguishing between cross talk and coactivation of neighboring muscles. It is possible that a high correlation between two surface EMG signals recorded over separate muscles may reflect a similarity in motor unit discharge patterns, for example due to motor unit synchronization, rather than a high level of cross talk between the muscles. Similarly, a low correlation between two signals does not necessarily indicate that they have originated in separate muscles, as a weak correlation can be observed even when cross talk from adjacent muscles is high.

REFERENCES

1. **Aagaard P, Simonsen EB, Andersen JL, Magnusson SP, Bojsen-Moller F, and Dyhre-Poulsen P.** Antagonist muscle coactivation during isokinetic knee extension. *Scand J Med Sci Sports* 10: 58–67, 2000.
2. **Andreassen S and Arendt-Nielsen L.** Muscle fibre conduction velocity in motor units of the human anterior tibial muscle: a new size principle parameter. *J Physiol* 391: 561–571, 1987.
3. **Andreassen S and Rosenfalck A.** Relationship of intracellular and extracellular action potentials of skeletal muscle fibers. *CRC Crit Rev Bioeng* 6: 267–306, 1981.
4. **Bremner FD, Baker JR, and Stephens JA.** Variation in the degree of synchronization exhibited by motor units lying in different finger muscles in man. *J Physiol* 432: 381–399, 1991.
5. **Buchthal F.** The general concept of the motor unit. *Neuromuscular disorders. Res Publ Assoc Res Nerv Ment Dis* 38: 3–30, 1961.
6. **Cesarelli M, Bifulco P, and Bracale M.** Study of the control strategy of the quadriceps muscles in anterior knee pain. *IEEE Trans Rehabil Eng* 8: 330–341, 2000.
7. **Clamann HP.** Statistical analysis of motor unit firing patterns in a human skeletal muscle. *Biophys J* 9: 1233–1259, 1969.
8. **De la Barrera EJ and Milner TM.** The effect of skinfold thickness on the selectivity of surface EMG. *Electroencephalogr Clin Neurophysiol* 93: 91–99, 1994.
9. **De Luca CJ and Erim Z.** Common drive in motor units of a synergistic muscle pair. *J Neurophysiol* 87: 2200–2204, 2002.
10. **De Luca CJ and Mambrito B.** Voluntary control of motor units in human antagonist muscles: coactivation and reciprocal activation. *J Neurophysiol* 58: 525–542, 1987.
11. **De Luca CJ, Le Fever RS, McCue MP, and Xenakis AP.** Control schemes governing concurrently active human motor units during voluntary contractions. *J Physiol* 329: 129–142, 1982.
12. **De Luca CJ and Merletti R.** Surface myoelectric signal cross-talk among the muscles of the leg. *Electroencephalogr Clin Neurophysiol* 69: 568–575, 1988.
13. **Dimitrov GV and Dimitrova NA.** Precise and fast calculation of the motor unit potentials detected by a point and rectangular plate electrode. *Med Eng Phys* 20: 374–381, 1998.
14. **Dimitrova NA, Dimitrov GV, and Nitkin OA.** Neither high-pass filtering nor mathematical differentiation of EMG signals can considerably reduce cross-talk. *J Electromyogr Kinesiol* 12: 235–246, 2002.
15. **Dorfman LJ, Howard JE, and McGill KC.** Motor unit firing rates and firing rate variability in the detection of neuromuscular disorders. *Electroencephalogr Clin Neurophysiol* 73: 215–224, 1989.
16. **Duchene J and Hogrel JY.** A model of EMG generation. *IEEE Trans Biomed Eng* 47: 192–201, 2000.
17. **Durnin JVGA and Womersley J.** Body fat assessed from total body density and its estimation from skinfold thickness: measurements on 481 men and women aged from 16 to 72 years. *Br J Nutr* 32: 77–97, 1974.
18. **Ebenbichler GR, Kollmitzer J, Glockler L, Bochdanský T, Kopf A, and Fialka V.** The role of the biarticular agonist and cocontracting antagonist pair in isometric muscle fatigue. *Muscle Nerve* 21: 1706–1713, 1998.
19. **Ekstedt J and Stalberg E.** Single fiber electromyography for the study of the microphysiology of the human muscle. In: *New Developments in Electromyography and Clinical Neurophysiology*, edited by Desmedt JE. Basel: Karger, 1973, p. 89–112.
20. **Enoka RM and Fuglevand AJ.** Motor unit physiology: some unresolved issues. *Muscle Nerve* 24: 4–17, 2002.
21. **Farina D and Merletti R.** A novel approach for precise simulation of the EMG signal detected by surface electrodes. *IEEE Trans Biomed Eng* 48: 637–646, 2001.
22. **Feinstein B, Lindegard B, Nyman E, and Wohlfart G.** Morphologic studies of motor units in normal human muscles. *Acta Anat (Basel)* 23: 127–142, 1955.
23. **Gabriel S, Lau RW, and Gabriel C.** The dielectric properties of biological tissues. III. Parametric models for the dielectric spectrum of tissues. *Phys Med Biol* 41: 2271–2293, 1996.
24. **Gootzen THJM, Stegeman DF, and Van Oosterom A.** Finite dimensions and finite muscle length in a model for the generation of electromyographic signals. *Electroencephalogr Clin Neurophysiol* 81: 152–162, 1991.
25. **Heymsfield SB, Mc Manus C, Smith J, Stevens V, and Nixon DW.** Anthropometric measurements of muscle mass: revised equations for calculating bone-free arm muscle area. *Am J Clin Nutr* 36: 680–690, 1982.
26. **Kleine BU, Stegeman DF, Mucd D, and Anders C.** Influence of motoneuron firing synchronization on SEMG characteristics in dependence of electrode position. *J Appl Physiol* 91: 1588–1599, 2001.
27. **Koh TJ and Grabiner MD.** Cross talk in surface electromyograms of human hamstring muscles. *J Orthop Res* 10: 701–709, 1992.

28. **Koh TJ and Grabiner MD.** Minimizing cross-talk in surface EMG. *J Biomech* 26: 151–157, 1993.
29. **Loeb GE and Gans C.** *Electromyography for Experimentalists*. Chicago, IL: University of Chicago Press, 1986.
30. **Lowery M, Stoykov N, Taflove A, and Kuiken TA.** A multiple-layer finite-element model of the surface EMG signal. *IEEE Trans Biomed Eng* 49: 446–454, 2002.
31. **Mangun GR, Mulkey RM, Young BL, and Goslow GE.** “Cross-talk” in electromyograms: contamination of EMGs recorded with bipolar fine-wire electrodes by volume conducted myoelectric activity from distant sources. *Electromyogr Clin Neurophysiol* 26: 443–461, 1986.
32. **Morrenhof JW and Abbink HJ.** Cross-correlation and cross-talk in surface electromyography. *Electromyogr Clin Neurophysiol* 25: 73–79, 1985.
33. **Powers RK, Vanden Noven S, and Rymer WZ.** Evidence of shared, direct input to motoneurons supplying synergist muscles in humans. *Neurosci Lett* 102: 76–81, 1989.
34. **Roeleveld K, Blok JH, Stegeman DF, and Van Oosterom A.** Volume conduction models for surface EMG; confrontation with measurements. *J Electromyogr Kinesiol* 7: 221–232, 1997.
35. **Rosenfalck P.** Intra and extracellular potential fields of active nerve and muscle fibers. *Acta Physiol Scand Suppl* 321: 1–168, 1969.
36. **Sears TA and Stagg D.** Short-term synchronization of intercostals motoneurone activity. *J Physiol* 480: 369–387, 1976.
37. **Semmler JG, Nordstrom MA, and Wallace CJ.** Relationship between motor unit short-term synchronization and common drive in human first dorsal interosseous muscle. *Brain Res* 767: 314–320, 1997.
38. **Sinderby C, Friberg N, Comtois N, and Grassino A.** Chest wall muscle cross-talk in canine costal diaphragm electromyogram. *J Appl Physiol* 81: 2312–2327, 1996.
39. **Snyder WS, Cook MJ, Karhausen LR, Nasset ES, Howells GP, and Tipton IH.** *International Commission on Radiological Protection No. 23*. Oxford, UK: Pergamon, 1974.
40. **Solomonow M, Baratta R, Bernadi M, Zhou B, Lu Y, Zhu M, and Acierno S.** Surface and wire EMG cross-talk in neighbouring muscles. *J Electromyogr Kinesiol* 4: 131–142, 1994.
41. **Solomonow M, Baratta R, Zhou BH, and D'Ambrosia R.** Electromyogram coactivation patterns of the elbow antagonist muscles during slow isokinetic movement. *Exp Neurol* 100: 470–477, 1988.
42. **Stoykov N, Lowery M, Taflove A, and Kuiken TA.** Frequency and time domain FEM models of EMG: capacitive effects and aspects of dispersion. *IEEE Trans Biomed Eng* 49: 763–772, 2002.
43. **Van Vugt JPP and van Dijk JG.** A convenient method to reduce crosstalk in surface EMG. *Clin Neurophysiol* 112: 583–592, 2001.
44. **Walpole RE and Myers RH.** *Probability and Statistics for Engineers and Scientists*. New York: Macmillan, 1989.
45. **Winter DA.** Electromyogram recording, processing, and normalization: procedures and considerations. *J Hum Muscle Perform* 1: 5–15, 1991.
46. **Winter DA, Fuglevand AJ, and Archer SE.** Crosstalk in surface electromyography: theoretical and practical estimates. *J Electromyogr Kinesiol* 4: 15–26, 1994.
47. **Wood JE, Meek SG, and Jacobsen SC.** Quantitation of human shoulder anatomy for prosthetic arm control. I. Surface modeling. *J Biomech* 22: 273–292, 1989.
48. **Yao W, Fuglevand AJ, and Enoka RM.** Motor unit synchronization increases EMG amplitude and decreases force steadiness of simulated contractions. *J Neurophysiol* 83: 441–452, 2000.